

# Nature-Inspired Photocatalytic Hydrogen Production with a Flavin Photosensitizer

Lucia Ivanová, Jan Truksa, Dong Ryeol Whang, Niyazi Serdar Sariciftci, Cigdem Yumusak,\* and Jozef Krajčovič\*



Cite This: *ACS Omega* 2024, 9, 5534–5540



Read Online

ACCESS |



Metrics & More

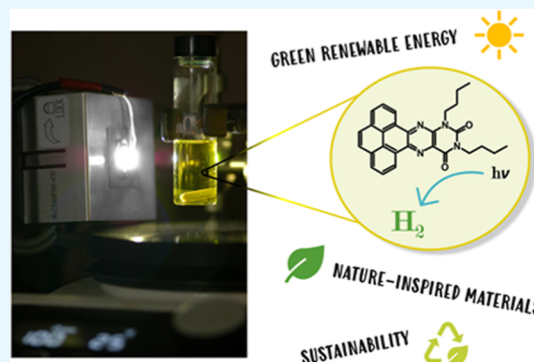


Article Recommendations



Supporting Information

**ABSTRACT:** Green hydrogen, by definition, must be produced with renewable energy sources without using fossil fuels. To transform the energy system, we need a fully sustainable production of green and renewable energy as well as the introduction of such “solar fuels” to tackle the chemical storage aspect of renewable energies. Conventional electrolysis of water splitting into oxygen and hydrogen gases is a clean and nonfossil method, but the use of massive noble-metal electrodes makes it expensive. Direct photocatalytic hydrogen evolution in water is an ideal approach, but an industrial scale is not available yet. In this paper, we intend to introduce flavins as metal-free organic photosensitizers for photoinduced reduction processes. Specifically, a flavin photosensitizer was employed for the photocatalytic evolution of hydrogen gas in aqueous media. The ratio of photosensitizer to cocatalyst concentration has been found to affect the efficiency of the hydrogen evolution reaction. Since flavins are nature-inspired molecules (like vitamin B2) with easily tunable properties through structure modification, this family of compounds opens the door for new possibilities in sustainable green hydrogen production.



## INTRODUCTION

Considering the prevalent use of fossil fuels, the increase in the amount of combustion emissions in the atmosphere, and the weather-dependent reliability of renewable sources (e.g., wind power plants), there is a need for emissionless fuel with a high energy density; the search for such nonfossil-based power sources is a top priority within the scientific community. In this context, hydrogen, whose production is powered by renewable energy without direct CO<sub>2</sub> emission (often referred to as green hydrogen), could become one of the alternative fuels of the future due to a high gravimetric energy density of 122 kJ g<sup>-1</sup>.<sup>1,2</sup> This could be a viable alternative to traditional energy storage methods for electrochemical batteries. In order to reach carbon neutrality in energy systems, the global production capacity for green hydrogen must increase by several orders of magnitude in the next decade.<sup>3</sup> This is a massive challenge, scientifically, technically, as well as politically.

Hydrogen today is produced by the reverse Sabatier reaction (using direct steam reforming and/or water gas shift reaction, etc.) by stripping the hydrogens from fossil methane gas. This is not sustainable and produces CO<sub>2</sub> in the process.

Conventional electrolysis of water splitting into oxygen and hydrogen gases is a clean and nonfossil method, but the use of massive noble metal electrodes makes it expensive.

Currently, the main process on the industrial scale is electrolytic hydrogen production by water splitting. Today, the electrical power for H<sub>2</sub> production by water electrolysis comes

mainly from nonrenewable fossil fuels, even in developed countries. If we address the question of the source of electrical power, electrification today is mostly based on fossil fuels, and then electrolysis is also fossil fuel-related and -dependent.

Furthermore, the main cocatalysts used therein, such as platinum, are often costly or toxic.<sup>4,5</sup> For these and many other reasons, looking for other effective alternative components for an environmentally friendly and fully renewable technology is necessary.

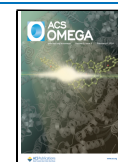
Direct photocatalysis has the advantage of directly utilizing solar energy, making it more ecologically valuable in remote places and small-scale applications. Today's drawback is that the overall conversion efficiency from “light energy converted into stored chemical energy” of direct photocatalysis is still lower than the indirect conversion using high-efficiency photovoltaics and subsequent electrocatalysis. That is scientifically a grand challenge to make direct photocatalysis more efficient. Many papers, books, and reports have been published in the last 50 years on the topic of “artificial photosynthesis”.<sup>2,6–9</sup>

**Received:** September 27, 2023

**Revised:** January 4, 2024

**Accepted:** January 11, 2024

**Published:** January 26, 2024



Prevalently, molecular-based  $H_2$ -evolving systems are multi-component. Arguably, the development of the photosensitizer is a considerable research challenge as it plays the important role of capturing initial solar irradiation and consequent photoexcited electron transfer through the system to a photochemically unreactive substrate. In the view of light harvesters, inorganic semiconductors (transition-metal oxides or hydroxides and their derivatives);<sup>10,11</sup> organic polymeric semiconductors;<sup>12</sup> graphitic materials;<sup>13</sup> metal–organic frameworks with photoresponsive metal ions surrounded with organic ligands;<sup>14</sup> organic dyes;<sup>15</sup> and organometallic complexes are several established divisions.<sup>16,17</sup> The value of the photosensitizer increases with the abundance of the material, good photostability and stability in neutral aqueous media, efficient working, and competitive cost.<sup>17,18</sup>

Biological photocatalytic processes like natural photosynthesis evolved over billions of years, resulting in the Calvin cycle combined with effective photosensitizer/photon converter photosystems (PS1 and PS2). For efficient photocatalysis, the active molecule should harvest as many photons in the visible region as possible.<sup>19</sup> This property is tunable in organic molecules via highest occupied molecular orbital (HOMO)/lowest unoccupied molecular orbital (LUMO) band gap engineering to fit the electrochemical window for a given process. Systems like  $TiO_2$  (3.2 eV band gap, UV-light irradiation) are much more challenging to modify to achieve a band gap alteration.<sup>20</sup> Eosin Y is frequently used as a photosensitizer, although its fast photodegradation causes problems.<sup>15,21</sup>

Alloxazines have attracted our attention as a part of the flavin family. Flavins are present in most biological systems, which take on diverse roles, from photosynthesis<sup>22</sup> to soil detoxification.<sup>23</sup> One outstanding example is vitamin B2, riboflavin,<sup>24,25</sup> which contains the isoalloxazine tautomeric core. The change in visible light absorption has been achieved by fusing aromatic molecules to the pteridine moiety or substituting the nitrogen atoms (see Figure 1).<sup>26,27</sup> While isoalloxazines are more frequent, the alloxazine isomer has superior photostability and a more straightforward synthesis. A

previous study<sup>28</sup> showed the variability of optical, electrochemical, and morphological properties of alloxazine derivatives. This property was applied by Golczak et al.<sup>29</sup> in a fluorescence microscopy study of human red blood cells. Presently, flavins are used for the photocatalysis of various oxidative reactions—the preparation of sulfoxides<sup>30</sup> or some cycloeliminations.<sup>31</sup>

Furthermore, previous electrochemical measurements performed by our group during studies of novel materials have shown favorable energy levels for hydrogen reduction. Because these molecules also have well-tunable visible-light absorption spectra, we have predicted using flavin-based systems for photocatalytic water splitting.<sup>28,32</sup>

Here in this paper, we report on utilizing novel fused flavin derivatives as photosensitizers for visible-light-driven hydrogen evolution reaction (HER). Our results open new possibilities in the realm of reductive photocatalysis, where the use of flavins remains rare 26.

## RESULTS AND DISCUSSION

The molar absorption coefficient of the flavin photosensitizer (FP) is  $10^5 \text{ M}^{-1} \text{ cm}^{-1}$  at  $\lambda_{\text{abs,max}} = 450 \text{ nm}$ , measured in the photocatalytic reaction solution (Figure 1) and suitable HOMO (−6.51 eV) and LUMO (−3.77 eV) levels indicating suitable band gap for use in artificial photosynthesis as a light harvester (Figure 2). To better describe the FP molecule, theoretical calculations were done using density functional theory (DFT) to find the stable molecular geometry and frontier orbital energies. Afterward, time-dependent (TD) DFT was used to calculate the electronic transitions. The calculations were performed in implicit tetrahydrofuran (THF) solvent. A strong theoretical HOMO/LUMO transition was found at 458 nm, with an oscillator strength of 0.30. An inspection of Figure 1, where this transition is shown by a red vertical line, shows a good fit of the TDDFT theoretical transition to the experiment. Other significant transitions, with an oscillator strength above 0.01, were found outside of the area of interest, i.e., outside the emission spectrum of the lamp, and are summarized in Table S1.

Furthermore, Figure 2 shows the energy levels of the FP measured by cyclic voltammetry (CV) and calculated in implicit  $CHCl_3$  solvent in a previous study.<sup>28</sup> Along with these, the presently calculated frontier molecular orbital (FMO) levels in THF are included. The FMO visualizations show the delocalization of the HOMO across the entire molecule, while the LUMO is located across the alloxazine moiety. In order to drive the reaction, the LUMO orbital of the photosensitizer must be above the redox potential of the  $H^+/H_2$  couple 19 (denoted as a green line in Figure 1). However, the FP molecule must perform two processes in the context of this reaction, i.e., excitation and charge transfer.

For an insight into the fundamentals and the mechanism of the process, we have decided on a partial water-splitting approach which required the use of a suitable electron-donating substance.<sup>18,33</sup> Because of the very large work function,<sup>34</sup> we have chosen platinum as the cocatalyst. Thus, the multicomponent catalytic system included a water-reduction cocatalyst (colloidal platinum) and TEA as a sacrificial electron donor (SD) to substitute the oxidation half-reaction. Even though the process is considered environmentally and economically unfavorable due to the requirement of SD consumption, it is useful to first examine photosensitizing properties straightforwardly before designing overall water-

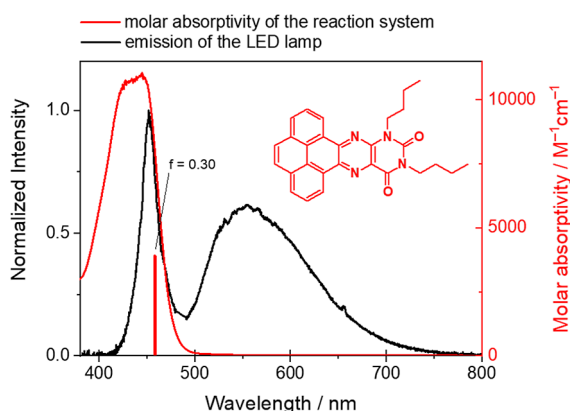


**Figure 1.** Molecular structure of the FP and the normalized spectrum of the light-emitting diode (LED) lamp used for irradiation, provided by the manufacturer—black, and the molar absorptivity of the reaction system containing FP (0.30 mM),  $K_2PtCl_4$  (0.05 mM), and 8:1:1 (v/v/v) of the THF/water/triethylamine (TEA) solution (10.0 mL in total)—red. The vertical red line shows the computed HOMO/LUMO transition in THF. The letter *f* denotes the oscillator strength of the transition.

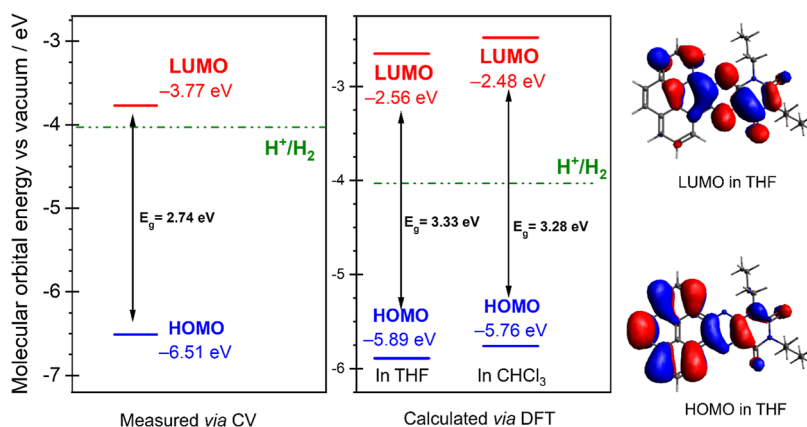


**Figure 2.** Energy of the FP's molecular orbitals from CV measurements [conditions: 1 mM FP in  $\text{CH}_2\text{Cl}_2$  with 0.1 M TBAPF<sub>6</sub> and 0.1 mM ferrocene (internal standard). Scan rate 200  $\text{mV}\cdot\text{s}^{-1}$  28] and TDDFT calculation in chloroform, and the computed MO energy levels in THF (corresponding to the optical HOMO/LUMO gap), along with visualizations of the orbitals. The green line shows the half-cell redox potential of  $\text{H}^+/\text{H}_2$  (green) =  $-4.03$  eV vs vacuum 19.

splitting systems.<sup>19,35</sup> Light-driven  $\text{H}_2$  evolution took place in a glass vial reactor (Figure 3) and was triggered by visible light

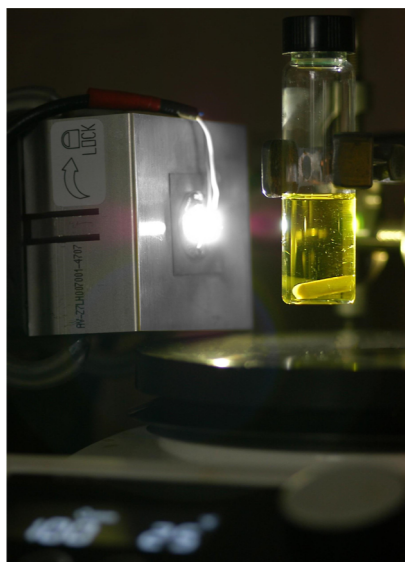


**Figure 3.** Picture of the reactor setup irradiated with an LED lamp.

irradiation ( $\lambda > 400$  nm) of the LED lamp. The emission spectrum of the lamp has a significant overlap with the FP's absorption spectrum (Figure 1).

Pilot experiments showed that the system is capable of  $\text{H}_2$  evolution, and blank experiments indicated that  $\text{H}_2$  evolution could not occur without the FP or cocatalyst. The FP molecular structure cannot provide an active site for the  $\text{H}_2$  reduction itself; therefore, the presence of a cocatalyst was necessary. Similarly, no  $\text{H}_2$  production occurred in the dark (see Figure S1), and the process clearly requires light initiation. Therefore, we feel justified in claiming that we have prepared a novel photocatalytic system for hydrogen production.

At first, experiments with different concentrations of cocatalyst  $\text{K}_2\text{PtCl}_4$  and FP were performed. By these experiments, the optimal cocatalyst concentration was revealed to be 0.05 mM. The optimal cocatalyst concentration was revealed by varying the  $\text{K}_2\text{PtCl}_4$  concentrations and vice versa. The measurements with different  $\text{K}_2\text{PtCl}_4$  concentrations are depicted in Figure 4-A. The maximum  $\text{H}_2$  evolution of 14.7  $\mu\text{mol}$  was achieved for 0.30 mM FP and 75  $\mu\text{M}$   $\text{K}_2\text{PtCl}_4$  after 2 h of irradiation. We have noticed a downturn at high platinum concentrations, which can be assigned to formation of the in situ-generated colloidal platinum aggregates, as is often discussed in the literature.<sup>36,37</sup> The  $\text{H}_2$  evolution dependence

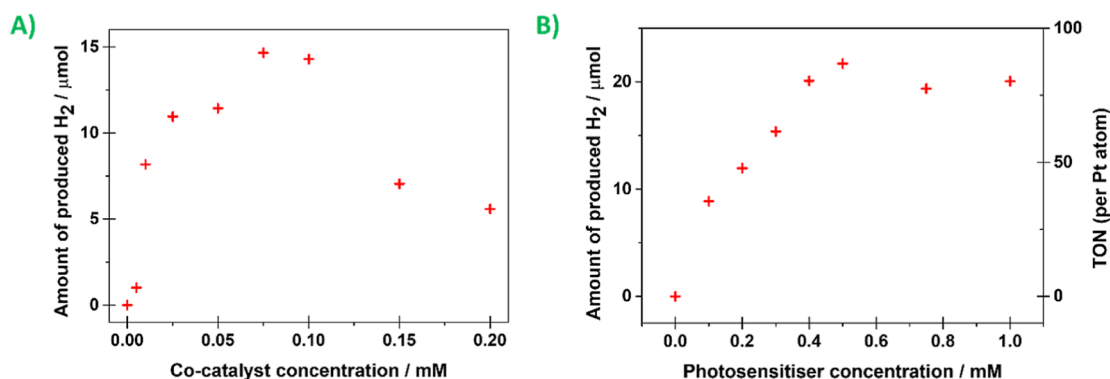


**Figure 4.** Photocatalytic measurements of 8:1:1 (v/v/v) of the THF/water/TEA solution (10.0 mL in total): (A) dependency of  $\text{K}_2\text{PtCl}_4$  cocatalyst concentration in the reaction systems containing FP (0.30 mM), during 2 h of irradiation to the light-driven hydrogen evolution; (B) dependency of FP concentration in the reaction systems containing  $\text{K}_2\text{PtCl}_4$  (0.05 mM), during 2 h of irradiation to the light-driven hydrogen evolution.

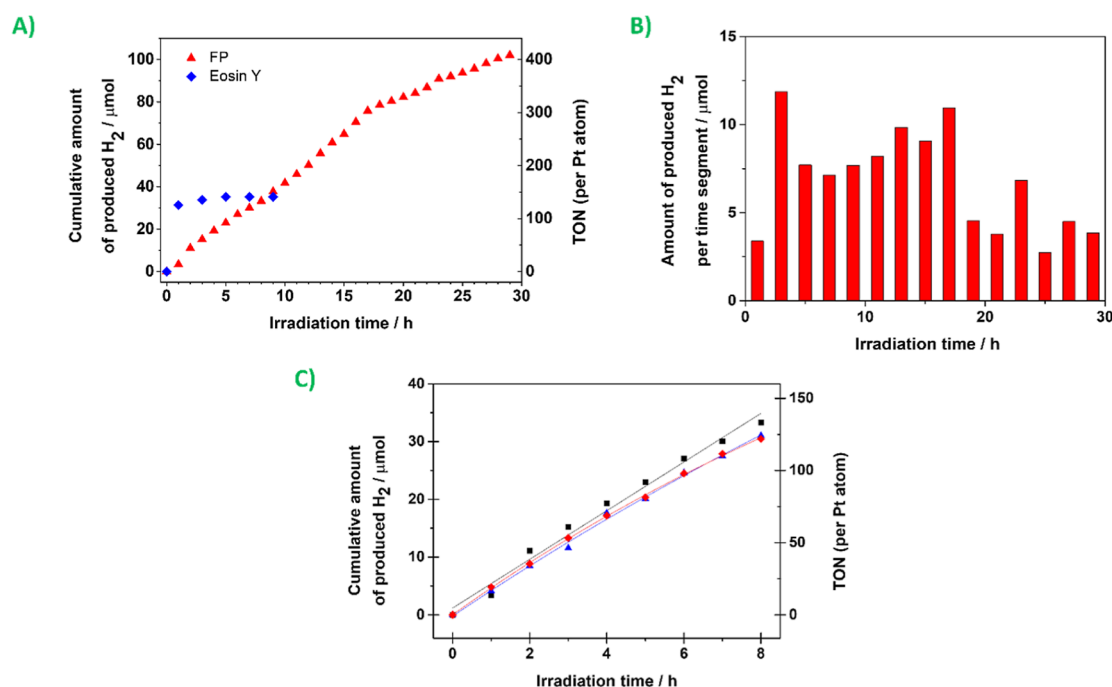


**Figure 5.** Photocatalytic measurements of the reaction system containing FP (0.30 mM),  $K_2PtCl_4$  (0.05 mM), and 8:1:1 (v/v/v) of the THF/water/TEA solution (10.0 mL in total): (A) time dependency of light-driven  $H_2$  evolution and (B) amount of  $H_2$  evolved per time segment during the same experiment; (C) three separated measurements of the time dependency during 8 h of irradiation.

on FP concentration is shown in Figure 4-B. The turnover number (TON) linearly increased with FP concentration and then reached 87 at 0.50 mM FP and saturated.

Further rise of the FP's amount had no significant effect on the  $H_2$  evolution. Probably, due to the fact that the light from the LED is absorbed, the excess FP has no way to affect the photolysis. However, at low FP concentrations, the  $H_2$  evolution is directly proportional to FP concentration, suggesting that the photolysis is FP-limited. To further illustrate this trend, Figure S2 shows the fit of Figure 4B with the equation  $H_2 = a(1 - 10^{-bx})$ , where  $a$  corresponds to a proportionality constant,  $b$  corresponds to the product of molar absorptivity ( $M^{-1} cm^{-1}$ ) and optical length of the reactor (cm), and  $x$  corresponds to the FP concentration (mM).

Regarding performance and cost efficiency, the optimal ratio of the FP to cocatalyst is 1:6 by 0.30 mM photosensitizer concentration. The TON was calculated based on the number of single-electron transfer processes using an equation

$$TON = \frac{2 \times n_{H_2}}{n_{Pt}}$$

where  $n_{H_2}$  represents the amount of evolved hydrogen ( $\mu mol$ ), and  $n_{Pt}$  represents the amount of the cocatalyst ( $\mu mol$ ).

Afterward, the photostability of the FP and reproducibility of the process within our system were studied. As a result, we have confirmed the steady  $H_2$  evolution for 29 h (Figure 5A). The aggregation of the cocatalyst possibly caused the visible decrease at the 18th hour, as we noticed a dark precipitate was formed (Figure 5B), which we considered to be the catalytically inactive platinum black.<sup>38,39</sup> After the experiment, the UV-vis measurement of the FP showed no significant changes to the pristine state. Therefore, we believe no photodegradation of the material occurred (see Figure S3).

Moreover, the photocatalytic properties of the FP were compared with Eosin Y, which showed rapid photodegradation, as previously documented,<sup>15,21</sup> followed by a consequent dramatic decrease in  $H_2$  evolution.

Last but not least, three simultaneous 8 h measurements (Figure 5C) were carried out that showed suitable reproducibility of the measurements.

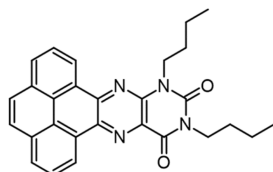
**Conclusions and Outlooks.** Our experiments demonstrate the use of a novel flavin derivative acting as a photosensitizer compared to Eosin Y for water splitting and HER. The system works with the highest efficiency when the concentration of the FP is 0.5 mM. The optimal cocatalyst  $K_2PtCl_4$  ratio was determined to be 1:6. This system was capable of continuous hydrogen production without a significant decline over 18 h, indicating sufficient photostability and reproducibility by repeated measurements. Moreover, we have proved that the system can work even under low irradiation in comparison to, e.g., the use of the solar simulator or xenon lamp.

These pilot experiments can serve as a springboard for future, more comprehensive work, which includes several other applications, such as the reduction of  $CO_2$  to methane or alcohols. Furthermore, to increase the attractiveness and competitiveness of photocatalytic processes, the reliance on sacrificial reagents will have to be eliminated to simplify the overall material balance and stop the use of potentially harmful chemicals.

**Experimental Section.** Commercially available chemicals were used as received.  $^1H$ - and  $^{13}C$  NMR spectra were recorded in  $CDCl_3$  using a Bruker AVANCE III 500 MHz spectrometer (Bruker, BioSpin GmbH, Germany) with working frequencies of 500 and 126 MHz, respectively, at 30 °C. Chemical shifts are expressed in parts per million ( $\delta$  scale) downfield from tetramethylsilane and are referenced to residual protium in the NMR solvent ( $CHCl_3$ :  $\delta$ 7.25 ppm).

Coupling constants ( $J$ ) are given in Hz with coupling expressed as d—doublet, dd—doublet of doublet, t—triplet, ddd—doublet of doublet of doublets, p—pentet, and m—multiplet. Melting points were determined using the Kofler apparatus with a microscope Nagma PHMK 05 (Nagma, Dresden, Germany).

**10,12-Dibutylpyreno[4,5-g]pteridine-11,13-(10*H*,12*H*)-dione (FP).**



**Molecular Mass:** 450.53 g·mol<sup>-1</sup>. <sup>1</sup>H NMR (CDCl<sub>3</sub>, 500 MHz):  $\delta$  9.30 (dd,  $J$  = 7.9, 1.4 Hz, 1H), 9.07 (dd,  $J$  = 8.2, 1.4 Hz, 1H), 8.62 (d,  $J$  = 8.2 Hz, 1H), 8.58 (dd,  $J$  = 8.2, 1.4 Hz, 1H), 7.86 (ddd,  $J$  = 8.2, 7.0, 1.4 Hz, 1H), 7.81–7.72 (m, 3H), 4.59–4.52 (m, 2H), 4.27–4.19 (m, 2H), 1.89 (p, 2H), 1.79 (p, 2H), 1.61–1.44 (m, 4H), 1.06 (t,  $J$  = 7.4 Hz, 3H), 1.01 (t,  $J$  = 7.4 Hz, 3H).

<sup>13</sup>C NMR (CDCl<sub>3</sub>, 126 MHz):  $\delta$  159.7, 150.4, 145.7, 144.0, 138.7, 131.3, 131.2, 130.0, 128.4, 128.2, 127.8, 127.7, 127.2, 127.0, 126.9, 126.7, 126.6, 124.8, 124.2, 123.7, 42.7, 42.5, 30.1, 29.9, 20.5, 20.4, 14.1, 14.0.

**Melting Point:** 240–241 °C. The irradiation was mediated by an MCPCB-Mounted MCWHD3 LED (Thorlabs, Newton, New Jersey, USA) with a typical output power of 2700 mW. The irradiance inside the glass vial was measured by using a Gigahertz-Optik X97 radiometer (probe calibrated for an interval of 400–800 nm). The irradiance value was 8.32 mW cm<sup>-2</sup>. Gaseous samples were taken using a gastight syringe equipped with a sampling syringe valve system (Hamilton Company, Reno, Nevada, USA). Gas chromatography analysis for H<sub>2</sub> was performed on a TRACE 1300 (Thermo Scientific, Waltham, Massachusetts, USA) with a 5 Å molecular sieve column (Thermo Scientific, Waltham, Massachusetts, USA), thermal conductivity detector (Thermo Scientific, Waltham, Massachusetts, USA), and nitrogen carrier gas. H<sub>2</sub> production was quantified from a one-point calibration of the H<sub>2</sub>/N<sub>2</sub> mixture.

The absorption spectra were measured using a SPECORD 50 PLUS UV–vis spectrophotometer (Analytik Jena, Jena, Germany). First, the absorption spectra were corrected to a baseline, which was determined by the measurement of absorption spectra of the THF/deionized water (8:1 ratio) solvent.

## MATERIALS AND SYNTHESIS

The molecule in question is the 10,12-dibutylpyreno[4,5-g]pteridine-11,13-(10*H*,12*H*)-dione further referred to as FP was prepared according to the procedure in ref 28, characterized with NMR and melting point measurements (summarized below) and used without further purification. All other solvents and reagents were obtained commercially and used without further purification.

**2 h Net Hydrogen Evolution Experiments.** A 25 mL photoreactor equipped with a magnetic stirrer and enclosed using a cap with a septum was filled with 10 mL of THF/deionized water (8:1) reaction solution containing various concentrations of the FP, various concentrations of K<sub>2</sub>PtCl<sub>4</sub>, and TEA (1 mL). The solution was degassed with nitrogen

and irradiated for 2 h. Afterward, a sample of the atmosphere was taken manually with a gastight syringe. All measurements were performed under oxygen-free conditions and at ambient temperature.

**TD H<sub>2</sub> Evolution Measurements.** A 25 mL photoreactor equipped with a magnetic stirrer and enclosed using a cap with a septum was filled with 10 mL of THF/deionized water (8:1) reaction solution containing various concentrations of the FP, various concentrations of K<sub>2</sub>PtCl<sub>4</sub>, and TEA (1 mL). The solution was degassed with nitrogen and was irradiated for an hour. Afterward, a sample of the atmosphere was taken manually with a gastight syringe. The degassing, irradiation, and sampling procedure was repeated for the same solution after every hour of the measurement. All measurements were performed under oxygen-free conditions and at ambient temperature.

**Blank Experiments with Irradiation.** A 25 mL photoreactor equipped with a magnetic stirrer and enclosed using a cap with a septum was filled with 10 mL of THF/deionized water (8:1) reaction solution containing either 0.3 mM FP and TEA (1 mL) or 0.05 mM K<sub>2</sub>PtCl<sub>4</sub> and TEA (1 mL). The solution was degassed with nitrogen and irradiated for 2 h. Afterward, a sample of the atmosphere was taken manually with a gastight syringe. All measurements were performed under oxygen-free conditions and at ambient temperature.

**Blank Experiments without Irradiation.** A 25 mL photoreactor equipped with a magnetic stirrer and enclosed using a cap with a septum was filled with 10 mL of THF/deionized water (8:1) reaction solution containing various concentrations of the FP, various concentrations of K<sub>2</sub>PtCl<sub>4</sub>, and TEA (1 mL). The solution was degassed with nitrogen and was left in the dark for 2, 5, 10, and 15 h. Afterward, a sample of the atmosphere was taken manually with a gastight syringe. All measurements were performed under oxygen-free conditions and at ambient temperature. The results of this experiment can be found in the Supporting Information (Figure S1).

## COMPUTATIONAL DETAILS

The quantum chemical calculations were performed using the Gaussian 16 program package<sup>40</sup> (see Table S1). The optimal geometries of the FP and Eosin Y were found via DFT calculation on the B3LYP<sup>41</sup> level of theory without any constraints (an energy cutoff of 10<sup>-5</sup> kJ mol<sup>-1</sup>, final RMS energy gradient under 0.01 kJ mol<sup>-1</sup> Å<sup>-1</sup>). Furthermore, the 6-31+G\*\* basis set was used<sup>42</sup> and proven effective in the past.<sup>43</sup> The density-based solvation model<sup>44</sup> was used to account for the solvent influence, while dispersion interactions were treated with Grimme's corrections (GD3BJ).<sup>45</sup> Since THF is the primary solvent in the mixture, it was used as the only solvent in the computations. Furthermore, the vertical singlet transition energies and oscillator strengths were found by using the TDDFT method with the lowest-energy conformations of the given molecules used as initial states. The potential energy surface minima were confirmed by inspecting the frequencies (no imaginary frequencies were found).

## ASSOCIATED CONTENT

### Supporting Information

The Supporting Information is available free of charge at <https://pubs.acs.org/doi/10.1021/acsomega.3c07458>.

Significant theoretical ground-state to excited-state transitions of the FP molecule, photocatalytic measurements of the reaction system in the dark, exponential fit of the amount of evolved hydrogen where  $a$  corresponds to a proportionality constant, and UV–vis of the FP before and after (recovered from the reaction system) (PDF)

## AUTHOR INFORMATION

### Corresponding Authors

**Cigdem Yumusak** – Linz Institute for Organic Solar Cells (LIOS), Institute of Physical Chemistry, Johannes Kepler University Linz, 4040 Linz, Austria; Phone: +43 732 2468 5847; Email: [cigdem.yumusak@jku.at](mailto:cigdem.yumusak@jku.at)

**Jozef Krajčovič** – Faculty of Chemistry, Brno University of Technology, CZ-612 00 Brno, Czech Republic; [orcid.org/0000-0002-7495-1787](https://orcid.org/0000-0002-7495-1787); Phone: +420541149433; Email: [krajcovic@fch.vut.cz](mailto:krajcovic@fch.vut.cz)

### Authors

**Lucia Ivanová** – Faculty of Chemistry, Brno University of Technology, CZ-612 00 Brno, Czech Republic; [orcid.org/0000-0002-0676-2386](https://orcid.org/0000-0002-0676-2386)

**Jan Truksa** – Faculty of Chemistry, Brno University of Technology, CZ-612 00 Brno, Czech Republic

**Dong Ryeol Whang** – Department of Advanced Materials, Hannam University, Daejeon 34430, Republic of Korea; [orcid.org/0000-0001-8402-2140](https://orcid.org/0000-0001-8402-2140)

**Niyazi Serdar Sariciftci** – Linz Institute for Organic Solar Cells (LIOS), Institute of Physical Chemistry, Johannes Kepler University Linz, 4040 Linz, Austria; [orcid.org/0000-0003-4727-1193](https://orcid.org/0000-0003-4727-1193)

Complete contact information is available at:  
<https://pubs.acs.org/10.1021/acsomega.3c07458>

### Notes

The authors declare no competing financial interest.

## ACKNOWLEDGMENTS

L.I. thanks the project FCH-S-23-8208 and Brno City Municipality (Ph.D. Talent) for financial support. Computational resources were provided by the e-INFRA CZ project (ID:90140), supported by the Ministry of Education, Youth and Sports of the Czech Republic. J.K. thanks the AKTION project no. 95p3.

## REFERENCES

- (1) Lam, M.; Lee, K. Renewable and sustainable bioenergies production from palm oil mill effluent (POME): Win–win strategies toward better environmental protection. *Biotechnol. Adv.* **2011**, *29* (1), 124–141.
- (2) *Hydrogen as a Future Energy Carrier*; Züttel, A., Borgschulte, A., Schlapbach, L., Eds.; Wiley, 2008.
- (3) Ehlers, J.; Feidenhans'l, A.; Therkildsen, K.; Larrazábal, G. O. Affordable Green Hydrogen from Alkaline Water Electrolysis: Key Research Needs from an Industrial Perspective. *ACS Energy Lett.* **2023**, *8* (3), 1502–1509.
- (4) Deshmukh, M.; Park, S.; Thorat, H.; Bodkhe, G.; Ramanavicius, A.; Ramanavicius, S.; Shirsat, M.; Ha, T. Advanced energy materials: Current trends and challenges in electro- and photo-catalysts for H<sub>2</sub>O splitting. *J. Ind. Eng. Chem.* **2023**, *119*, 90–111.
- (5) Jose, V.; Do, V.; Prabhu, P.; Peng, C.; Chen, S.; Zhou, Y.; Lin, Y.; Lee, J. Activating Amorphous Ru Metalenes Through Co

- Integration for Enhanced Water Electrolysis. *Adv. Energy Mater.* **2023**, *13*, 2301119.
- (6) Bozal-Ginesta, C.; Durrant, J. Artificial photosynthesis – concluding remarks. *Faraday Discuss.* **2019**, *215*, 439–451.
- (7) Whang, D.; Apaydin, D. Artificial Photosynthesis: Learning from Nature. *ChemPhotoChem* **2018**, *2* (3), 148–160.
- (8) Zhang, L.; Wang, Y. Decoupled Artificial Photosynthesis. *Angew. Chem., Int. Ed.* **2023**, *62* (23), No. e202219076.
- (9) Razeghifard, R. *Natural and Artificial Photosynthesis: Solar Power as an Energy Source*; Wiley, 2013.
- (10) Moss, B.; Lim, K.; Beltram, A.; Moniz, S.; Tang, J.; Fornasiero, P.; Barnes, P.; Durrant, J.; Kafizas, A. Comparing photoelectrochemical water oxidation, recombination kinetics and charge trapping in the three polymorphs of TiO<sub>2</sub>. *Sci. Rep.* **2017**, *7* (1), 2938.
- (11) Chen, S.; Takata, T.; Domen, K. Particulate photocatalysts for overall water splitting. *Nat. Rev. Mater.* **2017**, *2* (10), 17050.
- (12) Jayakumar, J.; Chou, H. Recent Advances in Visible-Light-Driven Hydrogen Evolution from Water using Polymer Photocatalysts. *ChemCatChem* **2020**, *12* (3), 689–704.
- (13) Bhandari, D.; Lakhani, P.; Modi, C. Graphitic carbon nitride (g-C 3 N 4) as an emerging photocatalyst for sustainable environmental applications: a comprehensive review. *RSC Sustain.* **2024**.
- (14) Dhakshinamoorthy, A.; Asiri, A.; García, H. Metal–Organic Framework (MOF) Compounds: Photocatalysts for Redox Reactions and Solar Fuel Production. *Angew. Chem., Int. Ed.* **2016**, *55* (18), 5414–5445.
- (15) Lewandowska-Andrałojć, A.; Larowska, D.; Gacka, E.; Pedzinski, T.; Marciniak, B. How Eosin Y/Graphene Oxide-Based Materials Can Improve Efficiency of Light-Driven Hydrogen Generation: Mechanistic Aspects. *J. Phys. Chem. C* **2020**, *124* (5), 2747–2755.
- (16) Wang, L. Recent Advances in Metal-Based Molecular Photosensitizers for Artificial Photosynthesis. *Catalysts* **2022**, *12* (8), 919.
- (17) Wang, M.; Han, K.; Zhang, S.; Sun, L. Integration of organometallic complexes with semiconductors and other nanomaterials for photocatalytic H<sub>2</sub> production. *Coord. Chem. Rev.* **2015**, *287*, 1–14.
- (18) Mazzeo, A.; Santalla, S.; Gaviglio, C.; Doctorovich, F.; Pellegrino, J. Recent progress in homogeneous light-driven hydrogen evolution using first-row transition metal catalysts. *Inorg. Chim. Acta* **2021**, *517*, 119950.
- (19) Kosco, J.; Moruzzi, F.; Willner, B.; McCulloch, I. Photocatalysts Based on Organic Semiconductors with Tunable Energy Levels for Solar Fuel Applications. *Adv. Energy Mater.* **2020**, *10* (39), 2001935.
- (20) Yan, H.; Wang, X.; Yao, M.; Yao, X. Band structure design of semiconductors for enhanced photocatalytic activity: The case of TiO<sub>2</sub>. *Prog. Nat. Sci.* **2013**, *23* (4), 402–407.
- (21) Alvarez-Martin, A.; Trashin, S.; Cuykx, M.; Covaci, A.; De Wael, K.; Janssens, K. Photodegradation mechanisms and kinetics of Eosin-Y in oxic and anoxic conditions. *Dyes Pigm.* **2017**, *145*, 376–384.
- (22) Zanetti, G.; Allverti, A. Ferredoxin: NADP+ Oxidoreductase. In *Chemistry and Biochemistry of Flavoenzymes*; Müller, F., Ed.; CRC Press, 2018, pp 305–316.
- (23) Dagley, S. Lessons From Biodegradation. *Annu. Rev. Microbiol.* **1987**, *41* (1), 1–24.
- (24) Butler, B.; Topham, R. Comparison of changes in the uptake and mucosal processing of iron in riboflavin-deficient rats. *Biochem. Mol. Biol. Int.* **1993**, *30* (1), 53–61.
- (25) Srivastava, V.; Singh, P.; Srivastava, A.; Singh, P. Synthetic applications of flavin photocatalysis: a review. *RSC Adv.* **2021**, *11* (23), 14251–14259.
- (26) *Flavin-Based Catalysis: Principles and Applications*, 1st ed.; Fraaije, M., Cibulka, R., Eds.; Wiley-VCH: Weinheim, 2021.
- (27) Klein, R.; Tatischeff, I. TAUTOMERISM AND FLUORESCENCE OF LUMAZINE. *Photochem. Photobiol.* **1987**, *45* (1), 55–65.

- (28) Richtar, J.; Ivanova, L.; Whang, D.; Yumusak, C.; Wielend, D.; Weiter, M.; Scharber, M.; Kovalenko, A.; Sariciftci, N.; Krajcovic, J. Tunable Properties of Nature-Inspired N,N'-Alkylated Riboflavin Semiconductors. *Molecules* **2020**, *26* (1), 27.
- (29) Golczak, A.; Insińska-Rak, M.; Davoudpour, A.; Hama Saeed, D.; Ménová, P.; Mojir, V.; Cibulka, R.; Khmelinskii, I.; Mrówczyńska, L.; Sikorski, M. Photophysical properties of alloxazine derivatives with extended aromaticity – Potential redox-sensitive fluorescent probe. *Spectrochim. Acta, Part A* **2022**, *272*, 120985.
- (30) Guo, H.; Xia, H.; Ma, X.; Chen, K.; Dang, C.; Zhao, J.; Dick, B. Efficient Photooxidation of Sulfides with Amidated Alloxazines as Heavy-atom-free Photosensitizers. *ACS Omega* **2020**, *5* (18), 10586–10595.
- (31) Hartman, T.; Reisnerová, M.; Chudoba, J.; Svobodová, E.; Archipowa, N.; Kutta, R.; Cibulka, R. *Photocatalytic Oxidative [2 + 2] Cycloelimination Reactions with Flavinium Salts: Mechanistic Study and Influence of the Catalyst Structure*. *ChemPlusChem* **2021**, *86* (3), 373–386.
- (32) Richtar, J.; Heinrichova, P.; Apaydin, D.; Schmiedova, V.; Yumusak, C.; Kovalenko, A.; Weiter, M.; Sariciftci, N.; Krajcovic, J. Novel Riboflavin-Inspired Conjugated Bio-Organic Semiconductors. *Molecules* **2018**, *23* (9), 2271.
- (33) Luo, G.; Pan, Z.; Lin, J.; Sun, D. Tethered sensitizer–catalyst noble-metal-free molecular devices for solar-driven hydrogen generation. *Dalton Trans.* **2018**, *47* (44), 15633–15645.
- (34) Xiao, N.; Li, S.; Li, X.; Ge, L.; Gao, Y.; Li, N. The roles and mechanism of cocatalysts in photocatalytic water splitting to produce hydrogen. *Chin. J. Catal.* **2020**, *41* (4), 642–671.
- (35) Pellegrin, Y.; Odobel, F. Sacrificial electron donor reagents for solar fuel production. *C. R. Chim.* **2017**, *20* (3), 283–295.
- (36) Lehn, J.; Sauvage, J. Chemical storage of light energy–catalytic generation of hydrogen by visible-light or sunlight-irradiation of neutral aqueous-solutions. *New J. Chem.* **1977**, *1*, 449–451.
- (37) Kiwi, J.; Grätzel, M. Hydrogen evolution from water induced by visible light mediated by redox catalysis. *Nature* **1979**, *281*, 657–658.
- (38) Quinson, J.; Jensen, K. From platinum atoms in molecules to colloidal nanoparticles: A review on reduction, nucleation and growth mechanisms. *Adv. Colloid Interface Sci.* **2020**, *286*, 102300.
- (39) Artero, V.; Fontecave, M. Solar fuels generation and molecular systems: is it homogeneous or heterogeneous catalysis? *Chem. Soc. Rev.* **2013**, *42* (6), 2338–2356.
- (40) Frisch, M.; Trucks, G.; Schlegel, H.; Scuseria, G.; Robb, M.; Cheeseman, J.; Scalmani, G.; Barone, V.; Petersson, G.; Nakatsuji, H.; Li, X.; Caricato, M.; Marenich, A.; Bloino, J.; Janesko, B.; Gomperts, R.; Mennucci, B.; Hratchian, H.; Ortiz, J.; Izmaylov, A.; Sonnenberg, J.; Williams-Young, D.; Ding, F.; Lipparini, F.; Egidi, F.; Goings, J.; Peng, B.; Petrone, A.; Henderson, T.; Ranasinghe, D.; Zakrzewski, V.; Gao, J.; Rega, N.; Zheng, G.; Liang, W.; Hada, M.; Ehara, M.; Toyota, K.; Fukuda, R.; Hasegawa, J.; Ishida, M.; Nakajima, T.; Honda, Y.; Kitao, O.; Nakai, H.; Vreven, T.; Throssell, K.; Montgomery, J.; Peralta, J.; Ogliaro, F.; Bearpark, M.; Heyd, J.; Brothers, E.; Kudin, K.; Staroverov, V.; Keith, T.; Kobayashi, R.; Normand, J.; Raghavachari, K.; Rendell, A.; Burant, J.; Iyengar, S.; Tomasi, J.; Cossi, M.; Millam, J.; Klene, M.; Adamo, C.; Cammi, R.; Ochterski, J.; Martin, R.; Morokuma, K.; Farkas, O.; Foresman, J.; Fox, D. *Gaussian 16*; Gaussian, Inc., 2016.
- (41) Lee, C.; Yang, W.; Parr, R. Development of the Colle-Salvetti correlation-energy formula into a functional of the electron density. *Phys. Rev. B: Condens. Matter Mater. Phys.* **1988**, *37* (2), 785–789.
- (42) Hariharan, P.; Pople, J. The influence of polarization functions on molecular orbital hydrogenation energies. *Theor. Chim. Acta* **1973**, *28* (3), 213–222.
- (43) Cagardová, D.; Truksa, J.; Michalík, M.; Richtár, J.; Weiter, M.; Krajčovič, J.; Lukeš, V. Spectroscopic behavior of alloxazine-based dyes with extended aromaticity: Theory vs Experiment. *Opt. Mater.* **2021**, *117*, 111205.
- (44) Marenich, A.; Cramer, C.; Truhlar, D. Universal Solvation Model Based on Solute Electron Density and on a Continuum Model

of the Solvent Defined by the Bulk Dielectric Constant and Atomic Surface Tensions. *J. Phys. Chem. B* **2009**, *113* (18), 6378–6396.

(45) Grimme, S.; Ehrlich, S.; Goerigk, L. Effect of the damping function in dispersion corrected density functional theory. *J. Comput. Chem.* **2011**, *32* (7), 1456–1465.

## Recommended by ACS

### Recent Progress in Nonsacrificial H<sub>2</sub>O<sub>2</sub> Generation Using Organic Photocatalysts and In Situ Applications for Environmental Remediation

Yanling Zhang, Yongfa Zhu, *et al.*

DECEMBER 15, 2023

ACCOUNTS OF MATERIALS RESEARCH

READ 

### Photocatalytic Transfer Hydrogenation Reactions Using Water as the Proton Source

En Zhao, Zupeng Chen, *et al.*

MAY 21, 2023

ACS CATALYSIS

READ 

### More Accurate Method for Evaluating the Activity of Photocatalytic Hydrogen Evolution and Its Reaction Kinetics Equation

Lan Zhou, Xueqing Qiu, *et al.*

FEBRUARY 21, 2023

LANGMUIR

READ 

### Anti-Dissipative Strategies toward More Efficient Solar Energy Conversion

Agustina Cotic, Alejandro Cadranel, *et al.*

FEBRUARY 15, 2023

JOURNAL OF THE AMERICAN CHEMICAL SOCIETY

READ 

Get More Suggestions >